

Acceleration of snow melt in an Antarctic Peninsula ice core during the twentieth century

Nerilie J. Abram^{1,2*}, Robert Mulvaney^{1*}, Eric W. Wolff¹, Jack Triest^{1,3}, Sepp Kipfstuhl⁴, Luke D. Trusel⁵, Françoise Vimeux⁶, Louise Fleet¹ and Carol Arrowsmith⁷

Over the past 50 years, warming of the Antarctic Peninsula has been accompanied by accelerating glacier mass loss and the retreat and collapse of ice shelves. A key driver of ice loss is summer melting; however, it is not usually possible to specifically reconstruct the summer conditions that are critical for determining ice melt in Antarctic. Here we reconstruct changes in ice-melt intensity and mean temperature on the northern Antarctic Peninsula since AD 1000 based on the identification of visible melt layers in the James Ross Island ice core and local mean annual temperature estimates from the deuterium content of the ice. During the past millennium, the coolest conditions and lowest melt occurred from about AD 1410 to 1460, when mean temperature was 1.6 °C lower than that of 1981–2000. Since the late 1400s, there has been a nearly tenfold increase in melt intensity from 0.5 to 4.9%. The warming has occurred in progressive phases since about AD 1460, but intensification of melt is nonlinear, and has largely occurred since the mid-twentieth century. Summer melting is now at a level that is unprecedented over the past 1,000 years. We conclude that ice on the Antarctic Peninsula is now particularly susceptible to rapid increases in melting and loss in response to relatively small increases in mean temperature.

Over the past decade, satellite monitoring has revealed that mass loss from the margins of the Antarctic and Greenland ice sheets is more pervasive than previously realized and represents a significant source of sea-level rise¹. A key driver of accelerated glacier outflow on these ice-sheet margins seems to be thinning and collapse of ice shelves. In some regions, such as the Amundsen Sea coast, ice-shelf thinning is being driven by basal melting from warm marine waters². On the Antarctic Peninsula, ice-shelf instability and loss has instead been linked to an increase in surface melting due to higher air temperatures in summer^{2–6}. Radar scatterometer data indicate that between 2000 and 2009 Antarctic Peninsula melt accounted for more than 50% of the total Antarctic surface melt intensity⁷, a finding supported by regional climate modelling of surface meltwater production over 1979–2010⁸.

Surface melting occurs in response to a positive energy balance after the snow surface temperature has warmed to its melting point. Several energy-balance components critical to melt are strongly correlated with air temperature⁹, and therefore the magnitude of above-freezing summer air temperatures is a well established proxy for melt intensity¹⁰. However, reconstructing the history of past summer temperature over Antarctica is difficult. Although stable-isotope records from ice cores can provide quantified reconstructions of mean temperature, the isotopic diffusion^{11,12} that occurs after snow deposition obscures the seasonal components except in the most highly resolved records. Instead, ice-core records of melt can be used to gain information about past summer temperatures and surface snow melt, using either the occurrence of melt layers at sites where melt is rare^{13–15} or the thickness of melt layers where melt occurs more frequently^{16,17}. Such ice-core melt records

have been used to reconstruct the history of summer melting at various sites across the Arctic^{15–17}; however, only one extended melt reconstruction so far exists for the Antarctic continent¹⁴.

In this study, we measure the annual melt intensity preserved in the James Ross Island (JRI) ice core^{18,19} and examine this alongside the ice-core isotope record of mean temperature change over the past 1,000 years. This first ice-core reconstruction of melt history for the Antarctic Peninsula is particularly valuable as it is derived from the region (Fig. 1a) where recent rapid atmospheric warming^{19,20} is believed to have increased ice melt, leading to widespread ice-shelf thinning and collapse^{3–5,21–23} and accelerated glacier mass loss^{24,25}.

Evaluating the ice-core proxies

The deuterium-isotope (δD) composition of the JRI ice core is used as a proxy for mean annual temperature at the ice-core site^{18,19}. Previous assessments against meteorological reanalysis data since 1979 show that the isotope signal contains summer and winter temperature information and is not biased on seasonal or interannual timescales by snow accumulation¹⁸. The ice-core δD record is significantly correlated with annual temperature measured at Esperanza Station ($r = 0.52$, $n = 56$, $p < 0.0001$; Fig. 1b). Esperanza is located close to sea level and approximately 100 km north of the JRI ice-core drill site. The mean annual temperature at Esperanza is -4.8°C , distributed around a winter (June–August) to summer (December–February) temperature range from -11.4°C to $+0.9^\circ\text{C}$ (1981–2000 interval). On the basis of borehole measurements, the temperature of the JRI ice cap at 10 m depth is -13.8°C . This suggests that the mean annual temperature at JRI is of the order of 9°C lower than at Esperanza. Similarly, using

¹British Antarctic Survey, Natural Environment Research Council, Cambridge CB3 0ET, UK, ²Research School of Earth Sciences, The Australian National University, Canberra, Australian Capital Territory 0200, Australia, ³UJF-Grenoble 1/CNRS Laboratoire de Glaciologie et Géophysique de l'Environnement (LGGE) UMR 5183, Grenoble F-38041, France, ⁴Alfred Wegener Institute for Polar and Marine Research, D-27568 Bremerhaven, Germany, ⁵Graduate School of Geography, Clark University, Worcester, Massachusetts 01610, USA, ⁶Institut de Recherche pour le Développement, Laboratoire HydroSciences Montpellier et Laboratoire des Sciences du Climat et de l'Environnement, 91191 Gif-sur-Yvette, France, ⁷NERC Isotope Geosciences Laboratory, British Geological Survey, Keyworth NG12 5GG, UK. *e-mail: nerilie.abram@anu.edu.au; rmu@bas.ac.uk.

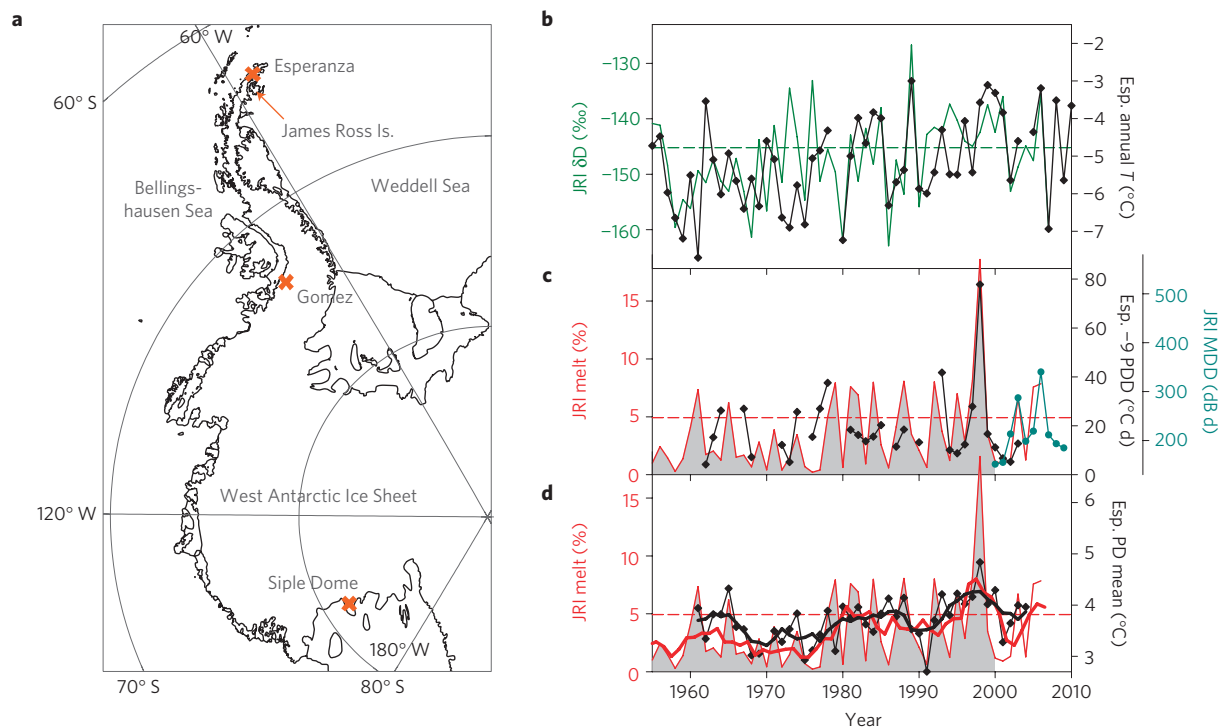


Figure 1 | Location and proxies. **a**, JRI lies near the northeastern tip of the Antarctic Peninsula. **b**, Mean annual (January–December) δD of the JRI ice core (green) and mean annual temperature at Esperanza (black). **c**, Annual (July–June) melt percentage at JRI (red), alongside QuikSCAT melt decibel-days for the JRI site (MDD; sum of backscatter exceeding melt threshold; cyan)⁷ and Esperanza annual PDD sum (black, daily data adjusted by -9°C). **d**, The same as in **c** but using PD mean (black). Dashed lines show 1981–2000 ice core means (**b–d**), bold curves are 5-year running means (**d**).

the altitudinal lapse rate of -0.58°C per 100 m observed on JRI (ref. 26) and across the Antarctic Peninsula²⁷, the ice-core site at 1,524 m elevation should be approximately 8.9°C lower than sea-level temperature in the area.

To examine how variability of melt intensity in the JRI ice core relates to positive summer temperatures we used daily observations of maximum temperature from Esperanza Station²⁸. We applied a -9°C offset to the Esperanza daily temperature data as a first-order estimate of the temperature difference between the ice-core site and Esperanza. We then calculated the annual (July–June) sum of all daily temperatures exceeding 0°C , known as the positive degree-day (PDD) sum^{13,14,29}. As the PDD parameter is based on a cumulative sum of daily temperatures we required daily data coverage greater than 90% during the summer months (December–February), resulting in many years where a reliable estimation of PDD was not possible. The mean of positive daily temperatures is a less precise parameter for describing melt than the PDD sum, but it is not systematically biased to lower values by missing data. Thus, the mean of daily temperatures exceeding 0°C (PD mean) in the Esperanza station data was also used as a more continuous observational record to compare with melt at JRI.

Visual melt layers in the JRI ice core were used to calculate melt intensity as the percentage of the annual water-equivalent accumulation that melted and refroze (Methods). The average melt intensity at JRI was 4.9% during the 1981–2000 interval, with a maximum annual melt of 18% recorded in the JRI ice core during the 1997/1998 summer (Fig. 1c). The annual percentage of melt at JRI has a significant positive correlation with PDDs calculated using the Esperanza station data ($r = 0.64$, $n = 32$, $p = 0.0001$). A clear correlation also exists between the PD mean and annual melt ($r = 0.53$, $n = 43$, $p = 0.0003$), as well as in their interannual variability illustrated by 5-year moving averages (Fig. 1d).

Further verification of the JRI melt record comes from its comparison with QuikSCAT radar scatterometer monitoring of

melting⁷. Although the scatterometer data only offer a short interval of overlap with the JRI record (2000–2007), they give continuous data coverage over this time and, unlike other longer satellite-derived melt records, they are sufficiently well resolved (effectively 8–10 km resolution)⁷ to isolate a melt signal for the summit of the JRI ice cap. The scatterometer data for JRI show that melt occurs at this site between October and March and is concentrated in the December–February summer months. Although the sample size is small, annual variability in scatterometer-derived melt is significantly correlated with melt intensity in the JRI ice core ($r = 0.81$, $n = 7$, $p = 0.027$; Fig. 1c) and, together with the Esperanza station data, confirms that the JRI ice core-melt record is representative of summer warmth inducing melt at this site.

Antarctic Peninsula climate during the twentieth century

To first characterize the spatial patterns of climate variability in this region, the JRI δD record of mean annual temperature was examined alongside similar annually resolved ice-core temperature records from the Antarctic Peninsula and the West Antarctic Ice Sheet^{30,31}. Using principal component (PC) analysis, the two leading modes of the ice-core array since AD 1900 highlight differences between recent warming on the West Antarctic Ice Sheet and the Antarctic Peninsula (Fig. 2). PC1 is the West Antarctic climate signal that is well documented for its significant warming in winter and spring^{32–34}, and more recently has been shown to also have a significant component of summer warming³⁵. Warming in this region has been attributed to increased advection of warm air masses onto continental West Antarctica caused by strengthening teleconnections with Pacific Ocean climate variability, focused particularly in the subtropical South Pacific convergence zone^{30,32–35} (Supplementary Fig. S1). The recent phase of warming over the West Antarctic Ice Sheet has been ongoing since the 1950s (Fig. 2c)³⁵, although with the length constraints of the current

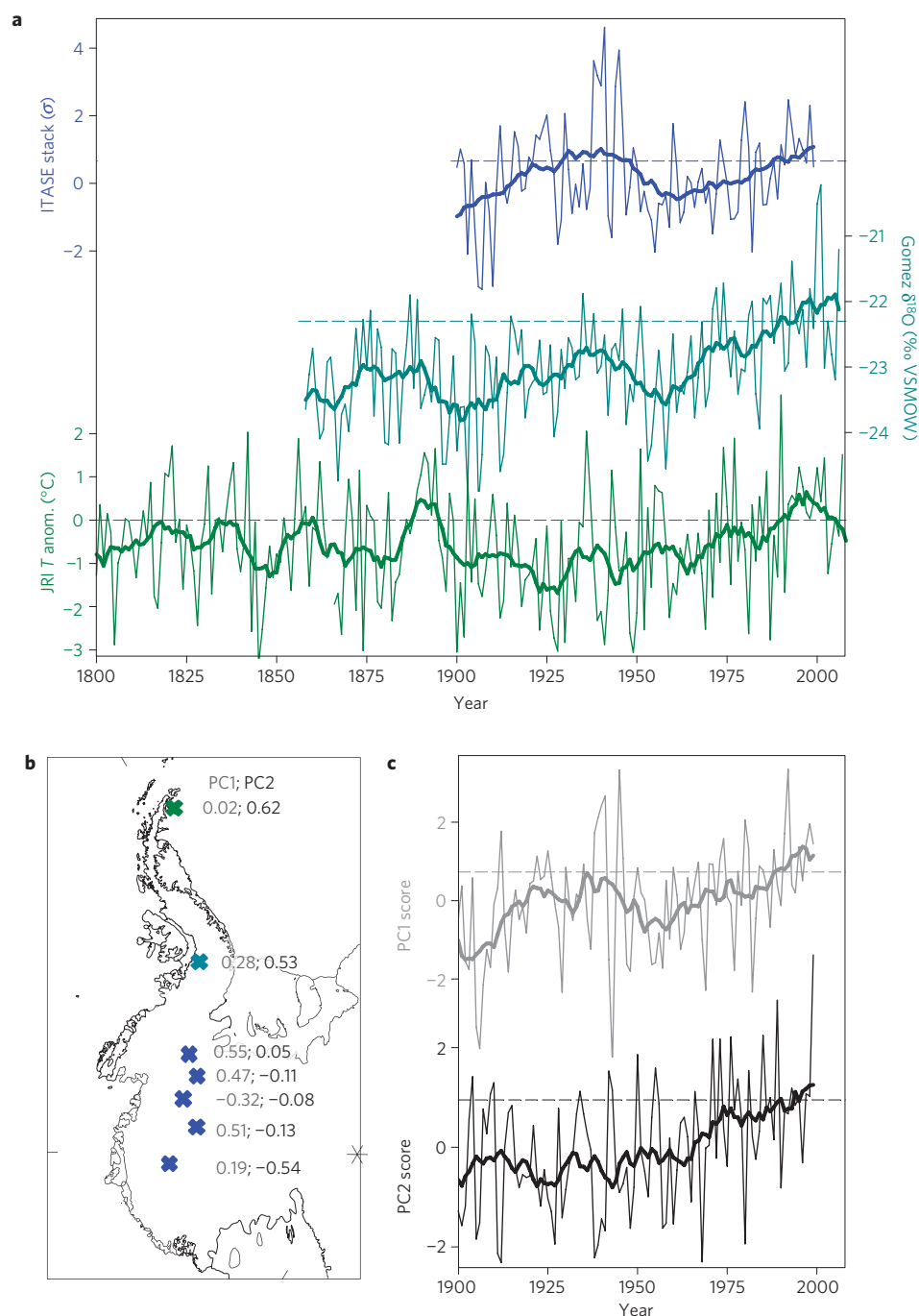


Figure 2 | Antarctic Peninsula and West Antarctic Ice Sheet warming. a, Mean annual (January–December) temperature reconstructions for JRI (green), Gomez (cyan)³¹ and a West Antarctica ice core stack (ITASE 01-5, 01-3, 01-2, 00-1 and 00-5; blue)³⁰. **b,c**, The seven ice core locations and their loadings (**b**) for the two leading modes of variability determined by PC analysis (**c**). PC1 (grey) is focused over West Antarctica, and PC2 (black) has a strong positive sign on the Antarctic Peninsula transitioning to negative on the Ross Sea side of West Antarctica. Dashed lines show 1981–2000 means; thick curves are 11-year running means (**a,c**).

ice-core records it is not possible to determine whether the strong multi-decadal variability in PC1 masks an earlier inception of the warming trend over the West Antarctic Ice Sheet. Recently, borehole temperature estimates from the West Antarctic Ice Sheet have provided evidence for a rapid acceleration of West Antarctic warming over the past two decades³⁶.

Antarctic Peninsula warming is captured by PC2 of the ice-core array (Fig. 2). The spatial composition of PC2 transitions from a strong positive contribution at JRI on the northern Antarctic Peninsula to a negative component on the Ross Sea

side of West Antarctica. Correlation of PC2 with ERA-Interim³⁷ 2 m temperature confirms this spatial pattern with opposing temperature anomalies focused over the Weddell and Amundsen–Ross sea regions (Fig. 3c). The correlation of PC2 with ERA-Interim sea-level pressure indicates that this temperature pattern is associated with pressure anomalies over the Antarctic continent and Amundsen Sea that are of opposite sign to the pressure anomalies within the mid-latitude band (Fig. 3b). This pressure pattern is characteristic of Southern Annular Mode³⁸ (SAM) circulation around the Antarctic continent, and is the leading mode of Southern

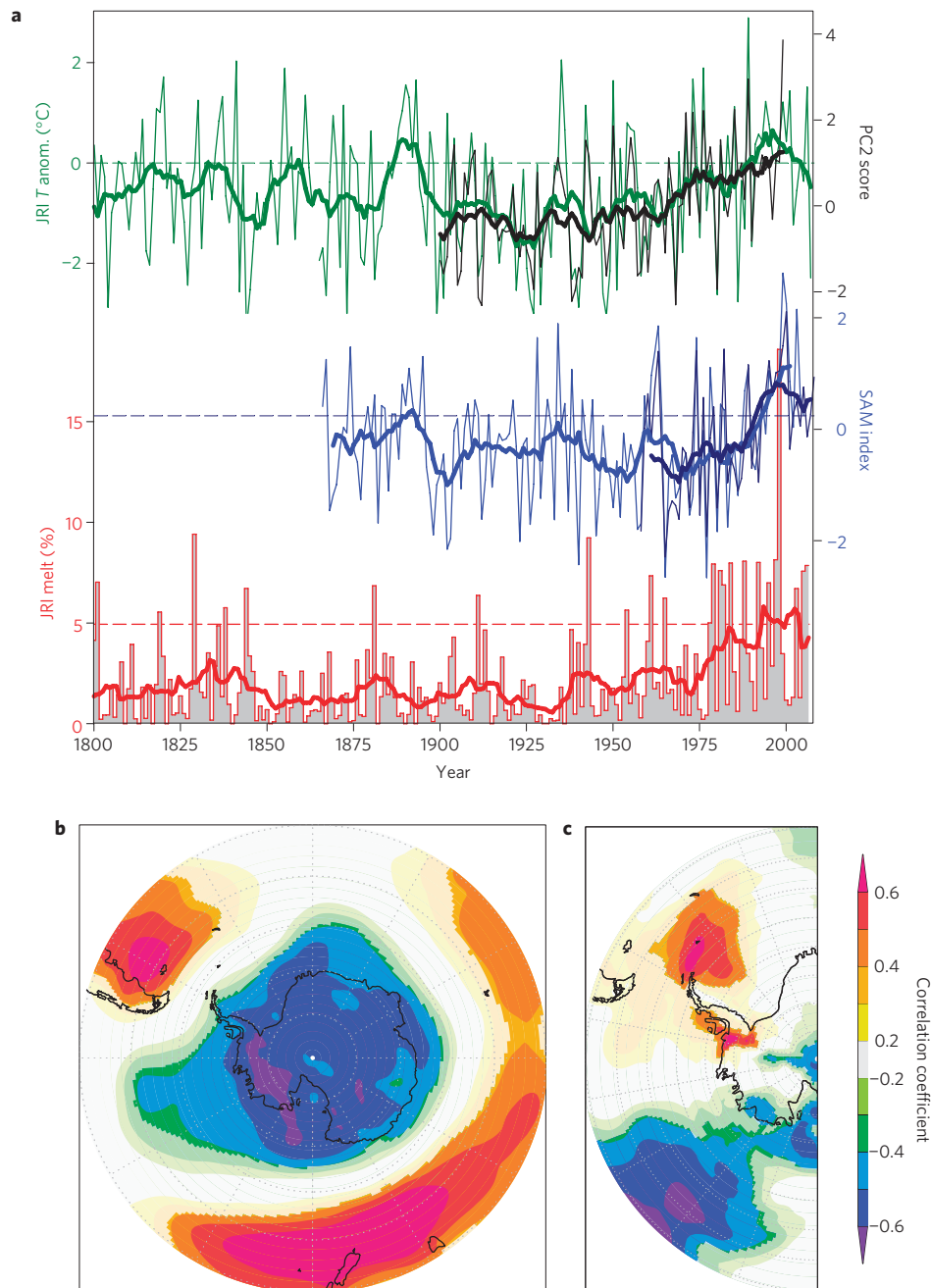


Figure 3 | Antarctic Peninsula climate variability. **a**, Mean annual (January–December) JRI temperature anomaly (green) and PC2 of the Antarctic Peninsula/West Antarctic ice core array (black) correlate with the SAM index in summer and autumn (ref. 38, dark blue; ref. 39, light blue; December–May averages shown). The annual (July–June) percentage of melt at JRI (red) increases coincident with twentieth-century warming. Thick lines show 11-year running means; dashed lines denote 1981–2000 means. **b,c**, The spatial correlation of PC2 with January to December annuals of ERA-Interim³⁷ mean sea-level pressure (**b**) and 2-m-temperature (**c**) supports SAM as a driver of the PC2 spatial temperature pattern. Dark shading shows correlations exceeding 90% confidence.

Hemisphere climate variability in the ERA-Interim reanalysis since 1979 (Supplementary Fig. S2). The role of the SAM on Antarctic Peninsula temperature variability during the twentieth century is further demonstrated by significant correlations of historical reconstructions of the SAM index^{38,39} with PC2 from the ice-core array and the JRI mean annual temperature record (Supplementary Table S1 and Fig. 3a). These correlations are strongest during the summer and autumn seasons.

The length of the JRI temperature reconstruction allows for a statistical assessment of when the recent rapid warming of the

Antarctic Peninsula was initiated. We examined this by filtering the 1,000-year annual temperature reconstruction across a range of filter widths to assess the significance of temperature trends in the record at different levels of smoothing⁴⁰ (Fig. 4, Methods). The inflection point of all filters between 15- and 40-year bandwidths indicates that the recent warming trend at JRI began around the 1920s (1928 ± 6 years; 2σ) and has been statistically significant (exceeding 90% confidence) since the 1940s (1942 ± 4 years). This warming is seen simultaneously in mean annual temperature and summer-melt intensity (Fig. 3a), suggesting a persistent summer

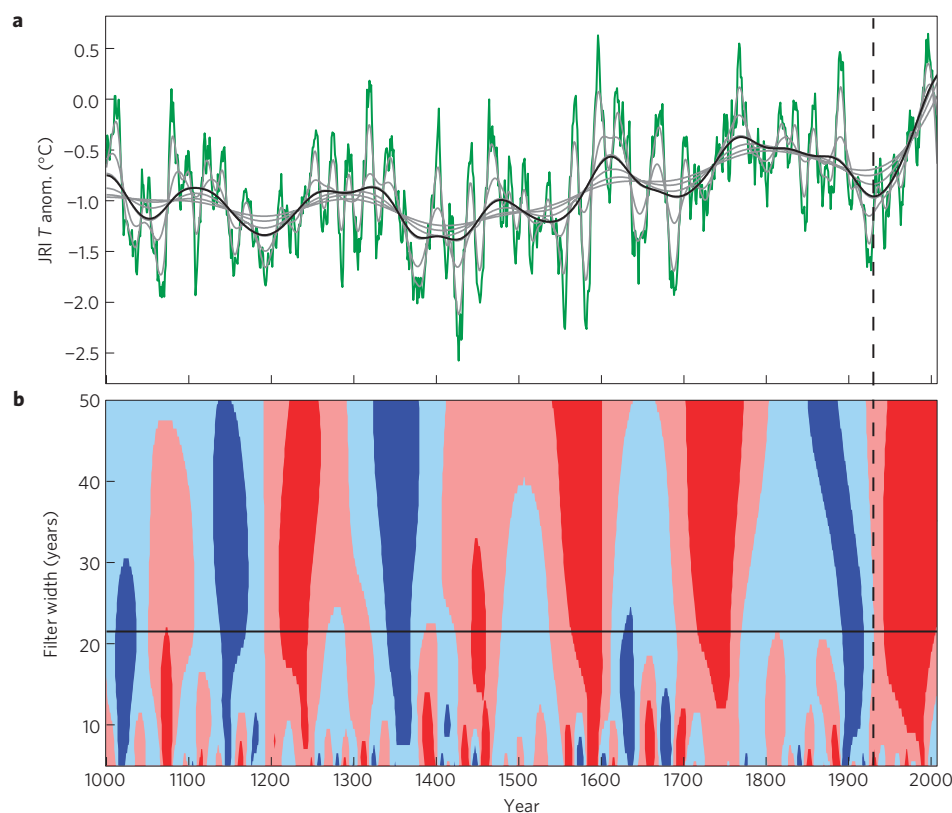


Figure 4 | Antarctic Peninsula temperature over the past millennium. **a**, 11-year moving average of JRI annual temperature anomaly (green) with Gaussian kernel smoothing filters at 5-, 10-, 20-, 30-, 40- and 50-year bandwidths (grey). **b**, A 21-year filter (black; **a**, **b**) provides the best data-driven filtering length determined using SiZer⁴⁰ to examine the significance of temperature trends across different filter lengths. Positive (and negative) trends are shown by red (and blue) shading, and dark shading indicates trends exceeding 90% confidence. The vertical dashed line (**a**, **b**) denotes the start of twentieth-century warming across 15–40-yr filter widths (1928 ± 6 years; 2σ).

component to Antarctic Peninsula warming during the twentieth century. These findings are in agreement with nearby station data indicating that warming at Orcadas (the only Antarctic site where climate observations span more than 100 years)⁴¹ has been significant since ~1950, and has been particularly strong in summer and autumn⁴².

Circulation changes associated with stratospheric ozone depletion have been widely discussed as a driver of summer strengthening of the SAM and associated recent warming on the Antarctic Peninsula⁴³. However, the mid-twentieth century start for significant warming of the Antarctic Peninsula is too early to be explained by the ozone depletion mechanism alone, and suggests that the early warming was influenced by other factors such as rising greenhouse-gas concentrations or natural variability that has since been reinforced by ozone-depletion-driven circulation changes^{41,44}. Our new constraints for the timing of recent warming at JRI will provide a valuable data set for assessing the ability of present climate models run under realistic transient forcings (including the Coupled Model Intercomparison Project Phase 5 (CMIP5) experiments) to simulate the twentieth-century progression of Antarctic Peninsula warming.

Temperature and ice melt over the past millennium

The coolest conditions at JRI over the past millennium occurred between ~AD 1410–1460, when mean temperature was 1.6°C lower than the 1981–2000 interval (Fig. 4). Warming since this time has occurred in progressive phases (Fig. 4b). As well as the warming since the mid-twentieth century, two intervals of significant warming also occurred between ~AD 1550–1600 and ~AD 1710–1760.

The JRI ice-core melt record has its minimum melt intensity for the past millennium between ~AD 1410 and 1460, coinciding with the coolest interval in mean annual temperature (Fig. 5). At this time, summer ice melt at JRI made up only 0.5% of the total accumulation. This represents a roughly tenfold lower melt intensity compared with the 4.9% melt observed for AD 1981–2000.

The history of melt intensity at JRI has visual similarities to the reconstruction of melt occurrence at Siple Dome¹⁴ on the West Antarctic Ice Sheet (Figs 1a and 5d). Both reconstructions show particularly low melt in the early fifteenth century, and that before the twentieth century the highest summer melting occurred during the sixteenth century. Interestingly, the sixteenth century is not characterized by similar warmth in the JRI mean annual temperature reconstruction, and borehole temperature information indicates that this was broadly a cool interval in West Antarctica³⁶. This implies that the high levels of melt on the Antarctic Peninsula and West Antarctic Ice Sheet during the sixteenth century were caused by an increased annual temperature range or increased interannual variability (that is, increased occurrence of warm summers and cool winters) rather than a warmer mean climate state.

The increase in summer melting at Siple Dome during the twentieth century is not as pronounced as at JRI. The Siple Dome record does not provide information on any melt that may have occurred since the ice core was drilled in 1999, so does not include a full response to the acceleration of West Antarctic warming in the past 20 years³⁶. However, the frequency of melt during the twentieth century (3 melt events) was clearly less than the melt frequency at this site during the sixteenth century (7 melt events). The principal component analysis of spatial temperature variability during the

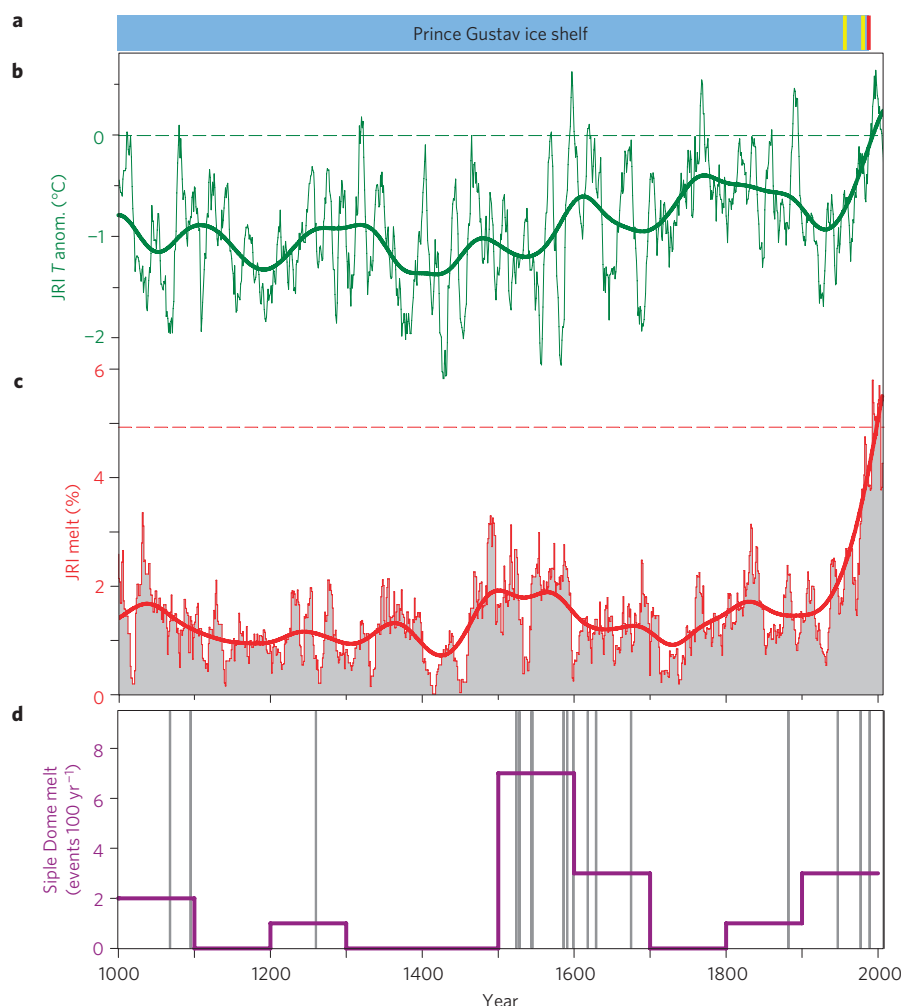


Figure 5 | Melt response over the past millennium. **a**, Schematic of Prince Gustav ice shelf history showing its presence (blue), intervals of rapid retreat (1957 and 1989; yellow) and collapse (1995; red)^{21,23}. **b,c**, JRI mean temperature anomaly (green; **b**) and melt percentage (red; **c**) shown as 11-year moving averages. Thick lines are 21-year Gaussian kernel filters; dashed lines denote 1981–2000 mean. Lowest temperatures and melt occurred at ~AD 1410–1460, followed by progressive warming and a nonlinear melt increase. **d**, The occurrence of melt layers (grey lines) and a 100-year stepped average of melt frequency (purple) at Siple Dome¹⁴ in West Antarctica.

twentieth century (Fig. 3 and Supplementary Fig. S2) indicated that the summer strengthening of the SAM that has caused at least part of the warming at the JRI site is also likely to have suppressed the rate of summer warming and melting (relative to strong winter and spring warming) in the Siple Dome region³⁵. Nevertheless, statistically significant summer warming of the West Antarctic Ice Sheet has now been detected, which is increasing the probability of future surface melting across the region³⁵.

The most striking difference between the mean annual temperature and melt histories from the JRI ice core over the past 1,000 years is the nonlinear characteristic of melt (Fig. 5). Mean annual temperature shows phases of progressive warming from ~AD 1460 to present day superimposed on a high degree of interannual to multidecadal variability, and the rate of warming over the past century has been shown to be highly unusual but not unprecedented in the context of natural climate variability¹⁹. In contrast, the JRI melt history shows more muted decadal-scale variability and its dominant feature over the past millennium is instead a sharp intensification since the mid-twentieth century to levels of melt that are unprecedented within the past 1,000 years.

The nonlinear response of melt to changes in mean temperature at JRI can be explained by the ~0 °C threshold of melting, meaning that in cooler conditions the ice-melt record loses the ability to

record variability in the surface energy balance and, by extension, summer temperatures. In addition, where summer temperatures do exceed the melting threshold, the amount of melt produced is proportional to the sum of the daily positive temperatures rather than their mean^{7,13}. This means that as average summer temperature increases and positive temperature days become warmer and more frequent, the amount of melt produced will exhibit an exponential increase^{29,45} (Supplementary Fig. S3). The strong summer component of twentieth-century warming on the Antarctic Peninsula also seems to have been critical in driving the unprecedented levels of melt here in recent decades, as the present mean annual temperature at JRI is not unprecedented within the scale of decadal variability at the site (Figs 3 and 5).

The combined JRI ice-core record of mean annual temperature and melt intensity provides a clear demonstration from the palaeoclimate record of the potential in the polar regions for nonlinear responses to future climate change. The nonlinearity of melt can help to explain how the relatively modest lowering of mean temperature at JRI in the late Holocene was sufficient to enable the establishment of a permanent ice shelf in Prince Gustav Channel^{19,23}, and also why this ice shelf apparently underwent rapid retreat and disintegration in the late twentieth century^{21,23} rather than gradual retreat during the centuries of progressive warming

since \sim AD 1460 (Fig. 5a). The nonlinearity of melt observed in the JRI ice-core record also highlights the particular vulnerability of areas in the polar regions where daily maximum temperatures in summer are close to 0°C and/or where summer isotherms are widely spaced, such as along the east and west coasts of the Antarctic Peninsula (Supplementary Fig. S3). In these places even modest future increases in mean atmospheric temperature could translate into rapid increases in the intensity of summer melt and in the poleward extension of areas where glaciers and ice shelves are undergoing decay caused by atmospheric-driven melting.

Methods

The JRI ice core was drilled 363.9 m to bedrock in January–February 2008 at $057^{\circ}41.10' \text{W}$, $64^{\circ}12.10' \text{S}$. Elevation at this site is 1,524 m, and mean water-equivalent accumulation is 0.63 m yr^{-1} (refs 18,19). The upper 200 years of the ice-core chronology is based on annual layer counting, using the well-defined annual cycle in non-sea-salt SO_4 (ref. 18). The annual-layer age scale is also constrained by fixed-time markers: a tephra layer from the 1967 Deception Island eruption, and the global SO_4 anomalies of the 1815 Tambora and 1809 Unknown eruptions^{18,19}. Beyond AD 1807, the age scale used here is the JRI-1 age scale, based on a glaciological flow model for the JRI site with an offset derived from 14 tephra horizons and the AD 1259 volcanic sequence¹⁹. The AD 1259 marker has an estimated uncertainty of ± 5 years and provides a firm age constraint for the past millennium of the JRI record that is examined here.

Analytical details for the measurement of the deuterium-isotope (δD) profile of the JRI core are described fully in ref. 19. Analytical precision on the δD measurements is typically 1.0‰ . The JRI δD data were averaged into annual bins to produce a record of mean δD in the ice core since AD 1000. Annual bins for the isotope data run from January–December and were selected to facilitate comparison with similar calendar-year annual isotope records from West Antarctic ice cores. A temperature dependence of $6.4\text{‰ }^{\circ}\text{C}^{-1}$ was used to derive a temperature history from the δD record at this site¹⁸. Temperature anomalies are calculated with respect to AD 1981–2000, which coincides with the time of rapid retreat and collapse of the adjacent Prince Gustav ice shelf²¹. Consistent temperature results are also produced by using $\delta^{18}\text{O}$ measured in the JRI ice core^{18,19}. An analysis of temperature trends over the past 1,000 years was carried out using the SiZer (Significant Zero crossing of derivatives) method⁴⁰ to calculate the significance of trends across different levels of smoothing. Smoothing was performed using a Gaussian kernel filter with bandwidths spanning all integer years in the range from 5 to 50 years. Assessments of the timing for the initiation of the twentieth-century warming trends use the mean and standard deviation of the change points in all filters between 15- and 40-year bandwidths so as to reduce the effect of high-frequency (interannual to decadal) variability on the change point estimates. The SiZer program was obtained at http://www.unc.edu/~marron/marron_software.html.

The presence and thickness of melt layers in the JRI ice core was determined using line-scan images of the core that were measured on the surface of 55-cm-long, 9.8-cm-wide and 3.3-cm-thick slabs cut during ice-core processing at Alfred Wegener Institute. The images were analysed for melt layers using a custom-built program in LabView software. To meet the classification of a melt layer^{13,14}, the melt feature had to be a layer of bubble-free ice with a sharp lower boundary that extended across at least 50% of the width of the core. Melt layers were common features in the ice core, although signs of large-scale melt percolation such as vertical melt pipes were not observed in the line-scan images. Supplementary Fig. S4 gives examples of line-scan images and melt assignment for three core pieces representing the near surface, mid-depth and deep portions of the melt record.

Melt layers were picked from the surface to a depth of 302.4 m. Beyond this, melt layers are still evident in the line-scan images of the JRI ice core; however, thinning of the annual ice layers by this depth made it uncertain that all layers would still be reliably detected. In this paper, we present the melt layer data back to AD 1000, which corresponds to a depth of 283.2 m in the JRI ice core and an annual layer thickness of 7.1 cm based on the JRI-1 chronology¹⁹. The position and thickness of the melt layers were used to calculate the percentage of the summer-centred (July–June) annual accumulation that was comprised of melt after conversion of both parameters to water-equivalent lengths¹⁷. Water equivalence of annual snow layers used a snow-water depth conversion based on density measurements along the length of the core, and for melt layer width used the 0.917 g cm^{-3} density of ice. Expressing melt as a percentage relative to annual accumulation, and assuming that ice-sheet thinning with depth affects melt layers in the same way as the annual water-equivalent layers, removes the need to apply a thinning correction to the melt thickness data¹⁷, which is desirable as thinning corrections become more uncertain with depth down an ice core. There is no long-term trend or deviation in the thinning-corrected annual accumulation at the JRI site over the 200 years spanning the annual chronology of the JRI core, indicating that the twentieth-century intensification of melt is not affected by its expression relative to annual layer thickness. An alternative method of quantifying melt (independently of annual layer thickness) as the annual sum of melt thickness

adjusted for thinning using the Nye equation⁴⁶ confirms that the results obtained for annual melt percentage are robust (Supplementary Fig. S5).

Data. The ice-core deuterium and melt data used in this study have been archived with the IGBP PAGES/World Data Centre for Paleoclimatology Data as Abram, N. J. *et al.* JRI ice core 1000 year deuterium and melt data, 2013. <ftp://ftp.ncdc.noaa.gov/pub/data/paleo/icecore/antarctica/james-ross-island/>.

Received 27 November 2012; accepted 4 March 2013;
published online 14 April 2013

References

- Pritchard, H. D., Arthern, R. J., Vaughan, D. G. & Edwards, L. A. Extensive dynamic thinning on the margins of the Greenland and Antarctic ice sheets. *Nature* **461**, 971–975 (2009).
- Pritchard, H. D. *et al.* Antarctic ice-sheet loss driven by basal melting of ice shelves. *Nature* **484**, 502–505 (2012).
- Scambos, T. *et al.* Ice shelf disintegration by plate bending and hydro-fracture: Satellite observations and model results of the 2008 Wilkins ice shelf break-ups. *Earth Planet. Sci. Lett.* **280**, 51–60 (2009).
- Scambos, T. A., Hulbe, C., Fahnestock, M. & Bohlander, J. The link between climate warming and break-up of ice shelves in the Antarctic Peninsula. *J. Glaciol.* **46**, 516–530 (2000).
- Van den Broeke, M. Strong surface melting preceded collapse of Antarctic Peninsula ice shelf. *Geophys. Res. Lett.* **32**, L12815 (2005).
- Barrand, N. E. *et al.* Trends in Antarctic Peninsula surface melting conditions from observations and regional climate modelling. *J. Geophys. Res.* <http://dx.doi.org/10.1029/2012JF002559> (2013).
- Trusel, L. D., Frey, K. E. & Das, S. B. Antarctic surface melting dynamics: Enhanced perspectives from radar scatterometer data. *J. Geophys. Res.* **117**, F02023 (2012).
- Kuipers Munneke, P., Picard, G., van den Broeke, M. R., Lenaerts, J. T. M. & van Meijgaard, E. Insignificant change in Antarctic snowmelt volume since 1979. *Geophys. Res. Lett.* **39**, L01501 (2012).
- Hock, R. Temperature index melt modelling in mountain areas. *J. Hydrol.* **282**, 104–115 (2003).
- Ohmura, A. Physical basis for the temperature-based melt-index method. *J. Appl. Meteorol.* **40**, 753–761 (2001).
- Cuffey, K. M. & Steig, E. J. Isotopic diffusion in polar firn: Implications for interpretation of seasonal climate parameters in ice-core records, with emphasis on central Greenland. *J. Glaciol.* **44**, 273–284 (1998).
- Johnsen, S. J. *et al.* in *Physics of Ice Core Records* (ed. Hondoh, T.) 121–140 (Hokkaido Univ. Press, 2000).
- Das, S. B. & Alley, R. B. Characterization and formation of melt layers in polar snow: Observations and experiments from West Antarctica. *J. Glaciol.* **51**, 307–312 (2005).
- Das, S. B. & Alley, R. B. Rise in frequency of surface melting at Siple Dome through the Holocene: Evidence for increasing marine influence on the climate of West Antarctica. *J. Geophys. Res.* **113**, D02112 (2008).
- Alley, R. B. & Anandakrishnan, S. Variations in melt-layer frequency in the GISP2 ice core: Implications for Holocene summer temperatures in central Greenland. *Ann. Glaciol.* **21**, 64–70 (1995).
- Fisher, D. *et al.* Recent melt rates of Canadian arctic ice caps are the highest in four millennia. *Glob. Plan. Change* **84–85**, 3–7 (2012).
- Herron, M. M., Herron, S. L. & Langway, C. C. Jr Climatic signal of ice melt features in southern Greenland. *Nature* **293**, 389–391 (1981).
- Abram, N. J., Mulvaney, R. & Arrowsmith, C. Environmental signals in a highly resolved ice core from James Ross Island, Antarctica. *J. Geophys. Res.* **116**, D20116 (2011).
- Mulvaney, R. *et al.* Recent Antarctic Peninsula warming relative to Holocene climate and ice-shelf history. *Nature* **489**, 141–144 (2012).
- Vaughan, D. G. *et al.* Recent rapid regional climate warming on the Antarctic Peninsula. *Climatic Change* **60**, 243–274 (2003).
- Cooper, A. P. R. Historical observations of Prince Gustav Ice Shelf. *Polar Rec.* **33**, 285–294 (1997).
- Domack, E. *et al.* Stability of the Larsen B ice shelf on the Antarctic Peninsula during the Holocene epoch. *Nature* **436**, 681–685 (2005).
- Pudsey, C. J., Murray, J. W., Appleby, P. & Evans, J. Ice shelf history from petrographic and foraminiferal evidence, Northeast Antarctic Peninsula. *Quat. Sci. Rev.* **25**, 2357–2379 (2006).
- Cook, A. J., Fox, A. J., Vaughan, D. G. & Ferrigno, J. G. Retreating glacier fronts on the Antarctic Peninsula over the past half-century. *Science* **308**, 541–544 (2005).
- Kunz, M. *et al.* Multi-decadal glacier surface lowering in the Antarctic Peninsula. *Geophys. Res. Lett.* **39**, L19502 (2012).
- Aristarain, A. J., Pinglot, J. F. & Pourchet, M. Accumulation and temperature measurements on the James Ross Island ice cap, Antarctic Peninsula, Antarctica. *J. Glaciol.* **33**, 357–362 (1987).

27. Reynolds, J. M. Distribution of mean annual temperatures in the Antarctic Peninsula. *Br. Antarct. Surv. Bull.* **54**, 123–133 (1981).
28. Tank, K. Daily dataset of 20th-century surface air temperature and precipitation series for the European Climate Assessment. *Int. J. Clim.* **22**, 1441–1453 (2002).
29. Braithwaite, R. J. in *Encyclopedia of Snow, Ice and Glaciers* (eds Singh, V. P., Singh, P. & Haritashya, U. K.) (Springer, 2011).
30. Schneider, D. P. & Steig, E. J. Ice cores record significant 1940s Antarctic warmth related to tropical climate variability. *Proc. Natl Acad. Sci. USA* **105**, 12154–12158 (2008).
31. Thomas, E. R., Dennis, P. F., Bracegirdle, T. J. & Franzke, C. Ice core evidence for significant 100-year regional warming on the Antarctic Peninsula. *Geophys. Res. Lett.* **36**, L20704 (2009).
32. Ding, Q. H., Steig, E. J., Battisti, D. S. & Kuttel, M. Winter warming in West Antarctica caused by central tropical Pacific warming. *Nature Geosci.* **4**, 398–403 (2011).
33. Schneider, D. P., Deser, C. & Okumura, Y. An assessment and interpretation of the observed warming of West Antarctica in the austral spring. *Clim. Dyn.* **38**, 323–347 (2012).
34. Steig, E. J. *et al.* Warming of the Antarctic ice-sheet surface since the 1957 International Geophysical Year. *Nature* **457**, 459–U454 (2009).
35. Bromwich, D. H. *et al.* Central West Antarctica among the most rapidly warming regions on Earth. *Nature Geosci.* **6**, 139–144 (2013).
36. Orsi, A. J., Cornuelle, B. D. & Severinghaus, J. P. Little Ice Age cold interval in West Antarctica: Evidence from borehole temperature at the West Antarctic Ice Sheet (WAIS) Divide. *Geophys. Res. Lett.* **39**, L09710 (2012).
37. Dee, D. P. *et al.* The ERA-Interim reanalysis: Configuration and performance of the data assimilation system. *Q. J. R. Meteorol. Soc.* **137**, 553–597 (2011).
38. Marshall, G. J. Trends in the southern annular mode from observations and reanalyses. *J. Clim.* **16**, 4134–4143 (2003).
39. Fogt, R. L. *et al.* Historical SAM Variability. Part II: Twentieth-Century Variability and Trends from Reconstructions, Observations, and the IPCC AR4 Models. *J. Clim.* **22**, 5346–5365 (2009).
40. Chaudhuri, P. & Marron, J. S. SiZer for exploration of structure in curves. *J. Am. Stat. Assoc.* **94**, 807–823 (1999).
41. Zazulie, N., Rusticucci, M. & Solomon, S. Change in climate at high southern latitudes: A unique daily record at Orcadas spanning 1903–2008. *J. Clim.* **23**, 189–196 (2010).
42. Marshall, G. J., Orr, A., van Lipzig, N. P. M. & King, J. C. The impact of a changing Southern Hemisphere Annular Mode on Antarctic Peninsula summer temperatures. *J. Clim.* **19**, 5388–5404 (2006).
43. Thompson, D. W. J. & Solomon, S. Interpretation of recent Southern Hemisphere climate change. *Science* **296**, 895–899 (2002).
44. Marshall, G. J. *et al.* Causes of exceptional atmospheric circulation changes in the Southern Hemisphere. *Geophys. Res. Lett.* **31**, L14205 (2004).
45. Vaughan, D. G. Recent trends in melting conditions on the Antarctic Peninsula and their implications for ice-sheet mass balance and sea level. *Arct. Antarct. Alp. Res.* **38**, 147–152 (2006).
46. Nye, J. F. Correction factor for accumulation measured by the thickness of the annual layers in an ice sheet. *J. Glaciol.* **4**, 785–788 (1963).

Acknowledgements

We thank our colleagues in the field, O. Alemany, S. Foord, S. Shelley and L. Sime, who took part in the ice-core drilling project; the Captain and crew of HMS *Endurance* who provided logistical support for the drilling field season; S. Foord, N. Lang, J. Levine, L. Sime, R. Röthlisberger, and the Alfred Wegener Institute at Bremerhaven for assistance in the processing of the ice core; and E. Capron, S. Foord and E. Ludlow for laboratory assistance. This study was aided by the use of the KNMI Climate Explorer web resource provided by G. J. van Oldenborgh, and we thank S. Das, H. Pritchard, J. King and C. Krause for helpful discussions during the preparation of the manuscript. This study is part of the British Antarctic Survey Polar Science for Planet Earth Programme, and was funded by the Natural Environment Research Council. Support from the Institut Polaire Français - Paul Emile Victor and the Institut National des Sciences de l'Univers in France, facilitated by J. Chappellaz and F. Vimeux, enabled the technical contribution of the French National Center for Drilling and Coring (INSU/C2FN). N.J.A. is supported by a Queen Elizabeth II fellowship awarded by the Australian Research Council (DP110101161).

Author contributions

R.M. led the project to drill the ice core, which also involved N.J.A. and J.T.; J.T. and S.K. performed the line-scan measurements and J.T. wrote the Labview software for melt analysis; N.J.A. and J.T. performed the melt layer analysis; N.J.A., R.M., L.F. and C.A. performed the chemical analysis; N.J.A. and R.M. developed the ice-core age scale; L.D.T. provided satellite melt data for JRI; N.J.A. led the data analysis and wrote the paper with contributions from R.M., E.W.W., L.D.T. and F.V.

Additional information

Supplementary information is available in the [online version of the paper](#). Reprints and permissions information is available online at www.nature.com/reprints. Correspondence and requests for materials should be addressed to N.J.A. or R.M.

Competing financial interests

The authors declare no competing financial interests.